Large-scale mapping observations of the CI 3P1-3P0 line toward heiles cloud2 in the Taurus Dark Cloud

LARGE-SCALE MAPPING OBSERVATIONS OF THE C I $^3P_1$–$^3P_0$ LINE TOWARD HEILES CLOUD 2 IN THE TAURUS DARK CLOUD

HIROYUKI MAEZAWA,[1] MASAFUMI IKEDA,[1] TETSUYA ITO,[1] GAKU SAITO,[1] YUTARO SEKIMOTO,[1,2] SATOSHI YAMAMOTO,[1]
KEN'ICHI TATEMATSU,[3] YUJI ARIKAWA,[4] YOSHIYUKI ASO,[3] TAKASHI NOGUCHI,[3] SHENG-CAI SHI,[3,5]
KEISUKE MIYAZAWA,[3] SHUJI SAITO,[6] HIROYUKI OZEKI,[6,7] HIDEO FUJIWARA,[6,8]
MASATOSHI OHISHI,[9] AND JUNJI INATANI[10]

ABSTRACT

A distribution of the neutral carbon atom (C I) in Heiles cloud 2 (HCL2) has been investigated with the Mount Fuji submillimeter-wave telescope. A region of 1.2 deg^2 covering a whole region of HCL2 has been mapped with the $^3P_1$–$^3P_0$ fine-structure line (492 GHz) of C I. The global extent of the C I emission is similar to that of ^{13}CO, extending from southeast to northwest. However, the C I intensity is found to be rather weak in dense cores traced by the J = 1–0 line of C^{18}O. On the other hand, strong C I emission is observed in a south part of HCL2 in which the C^{18}O intensity is fairly weak. The C I/CO abundance ratio is greater than 0.8 for the C I peak, whereas it is 0.1 for the dense cores such as the cyanopolyyne peak. The C I–rich cloud found in the south part may be in the early evolutionary stage of dense core formation where C I has not yet been converted completely into CO. This result implies that formation of dense cores is taking place from north to south in HCL2.

Subject headings: ISM: atoms — ISM: clouds — ISM: evolution — ISM: individual (Heiles's cloud 2)

1. INTRODUCTION

It has been established that dense cores in molecular clouds are formation sites of new stars since pioneering studies by P. C. Myers and his collaborators (e.g., Benson & Myers 1989). The evolution of a protostar born in a dense core has extensively been studied with observations in various wavelength regions from radio to X-ray. On the other hand, the formation process of a parent dense core is still poorly understood. The process will determine physical properties of a parent core, which are deeply related to the mass of a star to be born there. Therefore, it is of fundamental importance to investigate how dense cores are formed in molecular clouds.

Observations of the submillimeter-wave emission lines of the neutral carbon atom (C I) would provide us with new insight into the formation processes of dense cores. It is commonly thought that C I mainly exists in a relatively diffuse part of molecular clouds, called a photodissociation region (PDR). On the other hand, C I would also exist even in the interior of a dense core newly formed from the diffuse gas, since the conversion timescale of C I to CO is an order of the dynamical timescale of the core (~10^6 yr) according to chemical model calculations (Suzuki et al. 1992; Leung, Herbst, & Huebner 1984; Lee et al. 1996). Therefore, we would be able to investigate the formation process of dense cores by comparing the abundance distribution of C I with that of CO.

Heiles cloud 2 (HCL2; Heiles 1968) is a dark cloud in the Taurus region that is well-studied because of its proximity to the Sun (140 pc; Elias 1978). Since HCL2 is free from influences of nearby OB stars and supernova remnants, it is a good target for studying fundamental processes of dense core formation. This cloud involves several star-forming regions including the class 0 source, IRAS 04368+2557 in L1527, and also a famous source TMC-1, in which a number of long carbon-chain molecules have been detected (Kaifu et al. 1999; Ohishi, Irvine, & Kaifu 1991). Schloerb & Snell (1984) mapped a whole region of HCL2 with the ^{13}CO (J = 1–0) line and reported that HCL2 can be interpreted as a rotating ring. Cernicharo, Guélin, & Askne (1984) also proposed the ring structure of HCL2 on the basis of the visual extinction map. Cernicharo & Guélin (1987) clarified the distribution of dense gas in HCL2 by observations of C^{18}O, HCO$^+$, and H^{13}CO$^+$ and proposed that HCL2 consists of two bent filaments. More detailed ^{13}CO and C^{18}O observations in HCL2 were carried out in the course of a large-scale mapping observation in the Taurus region (Mizuno et al. 1995; Onishi et al. 1996, 1998). Recently, Sunada & Kitamura (1999) have made high spatial resolution observations of C^{18}O and ^{13}CO with the 45 m telescope of the Nobeyama Radio Observatory (NRO). As for the TMC-1 ridge, observations of various molecular lines have been made (e.g., Little et al. 1979; Olano, Walmsley, & Wilson 1988; Hirahara et al. 1992, 1995; Pratap et al. 1997) and a significant gradient in chemical abundances has been reported.

As for observations of the C I line, Schilke et al. (1995) reported a strip scan observation of the $^3P_1$–$^3P_0$ line with the Caltech Submillimeter Observatory (CSO) 10 m telescope. They made a five-point observation across the TMC-1 ridge and found that the C I intensity does not change very much from point to point. Tatematsu et al. (1999) have recently carried out a mapping observation of the limited area of HCL2

[1] Research Center for the Early Universe and Department of Physics, University of Tokyo, Tokyo 113-0033, Japan.
[2] Present address: Nobeyama Radio Observatory, National Astronomical Observatory of Japan, Nagano 384-1305, Japan.
[3] Nobeyama Radio Observatory, National Astronomical Observatory of Japan, Nagano 384-1305, Japan.
[4] Department of Astronomical Science, Graduate University for Advanced Studies, Nobeyama Radio Observatory, Nagano 384-1305, Japan.
[5] Present address: Purple Mountain Observatory, Nanjing, JiangSu 210008, China.
[6] Institute for Molecular Science, Okazaki 444-8585, Japan.
[7] Present address: National Space Development Agency of Japan, Tsukuba, Ibaraki 305-8505, Japan.
[8] Department of Chemical System Engineering, University of Tokyo, Tokyo 113-0033, Japan.
[9] National Astronomical Observatory of Japan, Mitaka, Tokyo 181-8588, Japan.
[10] National Space Development Agency of Japan, Tsukuba, Ibaraki 305-8505, Japan.

TABLE 1

LINE PARAMETERS AND COLUMN DENSITIES OF C I

Source	Offset (arcmin)	T_{MB}[a] (K)	ΔV[b] (km s^{-1})	$\int T_{MB}\,dV$ (K km s^{-1})	$N_{C\,I}/10^{17}$ (cm^{-2})	$N_{CO}/10^{18}$ (cm^{-2})	$N_{H_2}/10^{22}$ (cm^{-2})	$N_{C\,I}/N_{CO}$
TMC-1	(0, 0)	1.6 ± 0.2	1.9	2.9 ± 0.2	1.1–1.5	1.3–1.4	1.4–1.6	0.08–0.12
TMC-1C	(−3, 18)	1.4 ± 0.2	1.4	1.9 ± 0.3	0.6–1.0	0.9–1.0	1.0–1.1	0.06–0.11
C I peak	(6, −21)	2.4 ± 0.2	2.2	5.7 ± 0.3	>3.6	0.3–0.5	>0.66	>0.8
L1527	(−24, 21)	1.9 ± 0.3	2.1	3.9 ± 0.4	1.6–2.6	1.0–1.2	1.2–1.5	0.13–0.25
TMC-1A	(−30, 6)	1.7 ± 0.2	2.3	3.9 ± 0.3	1.6–2.2	1.7–1.8	1.9–2.0	0.09–0.13

[a] (0, 0) is taken at $\alpha(1950) = 04^h38^m38^s.6$, $\delta(1950) = 25°34'50''$.

[b] Corrected for the instrumental spectral resolution.

with the focal reducer system installed on CSO. They reported that the relatively constant C I intensity can be interpreted in terms of a picture of PDR. However, the mapping areas are quite small in these studies. This is because the C I emission from a cold dark cloud like HCL2 is generally weak (~2 K). As a result, no large-scale image of the C I emission has so far been obtained for any dark clouds including HCL2. It is essential to explore the distribution of C I in order to understand the formation process of dense cores. In this study, we report the first large-scale observation of C I toward HCL2 with the newly developed Mount Fuji submillimeter-wave telescope.

2. OBSERVATIONS

Observations of the $^3P_1$–$^3P_0$ line of C I (492.160651 GHz; Yamamoto & Saito 1991) toward HCL2 were carried out with the Mount Fuji submillimeter-wave telescope, which was installed at the summit of Mount Fuji (elevation 3724 m) in 1998 July. The diameter of the main reflector is 1.2 m, which gives the half-power beamwidth of 2'.2 at 492 GHz. The telescope is enclosed in a space frame radome with a GORE-TEX membrane in order to protect the telescope from wind and precipitation. The pointing of the telescope was calibrated by the continuum observations of the Sun and the Moon at 345 GHz every month, and the pointing accuracy is estimated to be 20'' (rms). The Moon efficiency including the radome attenuation was measured toward the full Moon to be 0.75 for 492 GHz. We have developed a 345 GHz/492 GHz dual band SIS mixer receiver. Parallel-connected twin junctions–type SIS mixers fabricated at NRO (Shi, Noguchi, & Inatani 1997) were employed in our receiver. We adopted a quasi-optical single sideband (SSB) system using two SIS mixers for the 492 GHz band (Inatani et al. 1998), whereas the 345 GHz mixer was operated in the double sideband (DSB) mode. The back end is an acousto-optical spectrometer (AOS) with a total bandwidth of 700 MHz. The frequency resolution of the spectrometer is 1.6 MHz, which corresponds to the velocity resolution of 1.0 km s^{-1} at the C I line frequency. The telescope system is operated remotely by using a commercial satellite communication system. Further details of the telescope will be described elsewhere (Sekimoto et al. 1999).

The submillimeter-wave observing conditions at Mount Fuji were found to be excellent in the winter season, as indicated by our previous 220 GHz radiometer measurements (Sekimoto et al. 1996). The zenith opacity at 492 GHz often became as low as 0.6. A typical system noise temperature was 1500 K (SSB) for 492 GHz and 500 K (DSB) for 345 GHz. Taking advantage of this good observing condition, we were able to observe a whole region of HCL2 with the grid spacing of 3'. The reference position was taken toward the cyanopolyyne peak of TMC-1 [$\alpha(1950) = 4^h38^m38^s.6$, $\delta(1950) = 25°35'45''$]. The number of total observing positions was 615. Observations were carried out in a position switch mode, where the off position was taken toward $\alpha(1950) = 4^h41^m38^s.6$, $\delta(1950) = 25°35'45''$. The on-source integration time was 100–300 s for each position depending on the sky condition, and the resultant rms noise temperature was about 0.2 K. The intensity was calibrated by using a chopper wheel method, where the difference between the absorber temperature and the sky temperature was taken into account. According to the calibration observations toward Ori KL, M17, and W3, the intensity scale should be reliable within 25%. Line parameters toward several representative positions are listed in Table 1. An example of the observed spectra is shown in Figure 1.

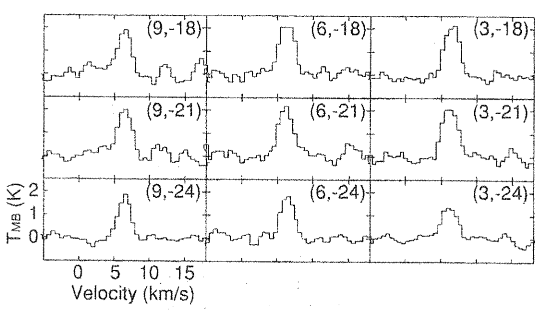

FIG. 1.—Example of the observed spectra of C I toward the C I peak. The offsets are given in arcminutes relative to the cyanopolyyne peak of TMC-1 at $\alpha(1950) = 4^h38^m38^s.6$, $\delta(1950) = 25°35'45''$.

3. DISTRIBUTION AND ABUNDANCE OF C I

The C I emission is detected in almost an entire region of HCL2. The observed brightness temperature is 1.6 K toward the cyanopolyyne peak of TMC-1. At this position, Schilke et al. (1995) reported the brightness temperature of C I to be 2.7 ± 0.5 K with the CSO 10 m telescope, and Tatematsu et al. (1999) reported it to be 1.6 K with the focal reducer experiment at CSO. Considering that the beam sizes are 10'' and 2' for observations by Schilke et al. (1995) and Tatematsu et al. (1999), respectively, our observational result toward the cyanopolyyne peak is consistent with the latter result. The line width corrected for the instrumental resolution of our AOS (1 km s^{-1}) is 1.9 km s^{-1} toward the cyanopolyyne peak, which is in good agreement with the previous reports. Figure 2 shows the integrated intensity map of C I in the HCL2 region. This is the first large-scale map of C I obtained toward a cold dark cloud. The overall extent of the emitting region of C I is comparable to those of ^{13}CO reported by Schloerb & Snell (1984) and by Sunada & Kitamura (1999). However, the detailed distribution of C I is significantly different from that of ^{13}CO within HCL2. This is in contrast to the previous observations. A good

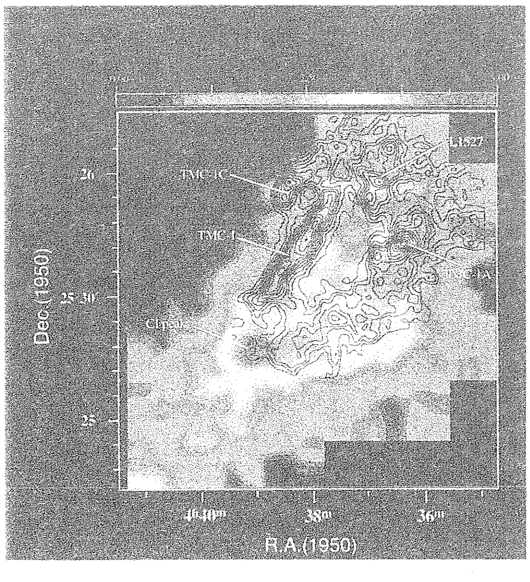

FIG. 2.—C I integrated intensity map of HCL2 (*color image*) superposed on the contour map of the $C^{18}O$ integrated intensity observed with the NRO 45 m telescope by Sunada & Kitamura (1999).

correlation between the C I emission and the ^{13}CO emission has been reported for giant molecular clouds (Plume et al. 1999; Ikeda et al. 1999). A similar correlation is suggested in a cold dark cloud, L183, based on the strip scan observation by Stark et al. (1996).

In Figure 2 the contour map of the $C^{18}O$ (J = 1–0) integrated intensity observed by Sunada & Kitamura (1999) is superposed on the map of C I. It is clear that the distribution of C I is remarkably different from that of $C^{18}O$; the C I intensity is generally weak in the dense core regions such as TMC-1, TMC-1A, TMC-1C, and L1527 that are prominent in $C^{18}O$. Particularly a ridge structure of TMC-1 is not seen in C I. On the other hand, the C I emission is the brightest in the southern part of HCL2, where the $C^{18}O$ and ^{13}CO emission is fairly weak (Sunada & Kitamura 1999). In this part, the maximum brightness temperature of C I is as high as 2.4 K. Thus, the C I distribution is globally anticorrelated with the $C^{18}O$ distribution.

The column density of C I is evaluated by using the method described by White, Casali, & Eiroa (1995). For simplicity we assume the LTE condition with the excitation temperature of 10 K, which is a typical kinetic temperature of dense cores (Benson & Myers 1989). This is justified because the C I line is well thermarized due to the low critical density of 10^3 cm^{-3}. At the cyanopolyyne peak, the column density averaged over our 2.′2 beam is determined to be (1.1–1.5) × 10^{17} cm^{-2}. Schilke et al. (1995) reported the lower limit of the column density to be 10^{17} cm^{-2}, and hence, our estimate is almost consistent with theirs. At the C I peak, the C I column density is determined to be greater than 3.6 × 10^{17} cm^{-2}. The estimated optical depth of the C I line is larger than 2.2 at the C I peak, whereas it is 0.9–1.3 at the cyanopolyyne peak. We also derived the column density of C I toward three dense cores: TMC-1C, L1527, and TMC-1A. The result is summarized in Table 1.

The column density of $C^{18}O$ is derived under an assumption that the J = 1–0 line of $C^{18}O$ is optically thin and the excitation temperature is 10 K. The $C^{18}O$ column density is determined to be (2.6–2.8) × 10^{15} cm^{-2} and (6.0–9.2) × 10^{14} cm^{-2} for the cyanopolyyne peak and the C I peak, respectively. When we assume the terrestrial ratio, 500, for the CO/$C^{18}O$ abundance ratio, the C I/CO abundance ratio is evaluated to be 0.08–0.12 and greater than 0.8 for the cyanopolyyne peak and the C I peak, respectively. In a similar way, the C I/CO abundance ratio for other dense cores (TMC-1C, L1527, and TMC-1A) is derived as listed in Table 1. The C I/CO abundance ratio at the C I peak is higher than those of dense cores including the cyanopolyyne peak by an order of magnitude. The C I/CO abundance ratio observed at the C I peak is slightly smaller than those observed for translucent clouds, 3–6 in HD 210121 (Stark & van Dishoeck 1994) and 0.4–2.5 in the southern hemisphere high-latitude clouds (Ingalls et al. 1997).

These results are not seriously affected by the assumption of the excitation temperature as far as it is higher than 10 K. When we assume the excitation temperature of 15 K for both the C I and $C^{18}O$ lines, the C I/CO abundance ratio is derived to be 0.03–0.04 and 0.2–0.4 for the cyanopolyyne peak and the C I peak, respectively. If the excitation temperature is much lower than 10 K, the optical depth of the C I line might be very thick. In this case, the observed intensity variation represents the temperature distribution of the cloud surface. However, this would not be the case for the reason mentioned before.

4. FORMATION OF DENSE CORES IN HCL2

We have found a clear anticorrelation between the C I and $C^{18}O$ distributions. In the dense core regions TMC-1, TMC-1A, TMC-1C, and L1527, the $C^{18}O$ emission is intense, whereas the C I integrated intensity is rather weak. This indicates that most of the C I has already been converted to CO in the dense core regions. In fact, the C I/CO abundance ratio is around 0.1 toward the cyanopolyyne peak of TMC-1. In dense core regions, the C I emission seems to originate from a surface layer of the clouds illuminated by the interstellar UV radiation field, as suggested by Tatematsu et al. (1999).

In our observations, we found the C I–rich cloud at the southern part of HCL2. This part shows the relatively large visual extinction ($A_v > 6$) according to the star count data (Cernicharo & Guélin 1987). This indicates that the H_2 column density toward the C I peak is larger than 6 × 10^{21} cm^{-2}. In fact, a sum of the column densities of C I and CO at the C I peak is larger than 6.6 × 10^{17} cm^{-2}. If the abundance of C I plus CO relative to H_2 is assumed to be 10^{-4}, the H_2 column density is roughly estimated to be greater than 6.6 × 10^{21} cm^{-2}, which is consistent with the above estimate from the visual extinction. This value is almost comparable to the H_2 column density toward the cyanopolyyne peak (1.5 × 10^{22} cm^{-2}). Such a high column density is further supported by bright *IRAS* 100 μm emission toward the C I–rich cloud. Therefore it seems to be difficult that the high C I/CO abundance ratio at the C I peak is interpreted in terms of a simple PDR model.

The total mass of C I–rich cloud is roughly estimated to be larger than 50 $M_\odot$ from the derived column density. This value is almost comparable to the mass of the TMC-1 ridge, 20–40 $M_\odot$ (Pratap et al. 1997; Snell, Langer, & Frerking 1982). If the line-of-sight distance of the C I–rich cloud is comparable to its apparent size, 0.4 pc, the mean density of the C I–rich cloud is higher than 5.4 × 10^3 cm^{-3}. The mean density derived above is comparable to or slightly lower than those for dense cores (Benson & Myers 1989).

We note that three T Tauri stars (LkHα 332/G1, LkHα 332/

G2, V955 Tau) are close to the C I peak (Itoh, Tamura, & Gatley 1996; Itoh, Tamura, & Nakajima 1999). However, the UV flux expected at 0.01 pc distance from the T Tauri star is estimated to be an order of magnitude smaller than the general interstellar UV radiation, and hence its contribution to the C I peak would be negligible. In addition, more than 30 young stellar objects (YSOs) are distributed over the HCL2 region, reflecting the past star formation activities, and the distribution of C I seems to have no correlation to that of YSOs.

There are at least two possibilities that account for the C I–rich cloud. The first possibility is that the cloud has a clumpy structure that allows the interstellar UV radiation to penetrate into deep inside of the cloud. This idea has been invoked to explain strong C II emission from molecular cloud cores (Stutzki et al. 1988; Burton, Hollenbach, & Tielens 1990) and has also been proposed to account for wide distribution of the C I emission (Genzel et al. 1988; Boissé 1990; Spaans et al. 1996). In this case, there should be a significant difference in the clumpy structure between the C I–rich cloud and dense cores, since the C I/CO abundance ratio is much higher in the C I–rich cloud. Another possibility is that the cloud is in the early stage of chemical evolution (Suzuki et al. 1992). A timescale for conversion from C I into CO is comparable to the dynamical timescale, and hence, C I can be abundant for a while even after interstellar UV radiation is shielded. Therefore, the C I/CO abundance ratio is expected to be high in the early stage of chemical evolution, whereas it becomes lower in the later stage. The C I/CO abundance ratio observed toward the C I–rich cloud is just intermediate between that for dense cores and that for translucent clouds. Considering that the mass and density of the C I–rich cloud, it seems reasonable that the cloud is in the early stage and C I has not been converted completely into CO in the C I–rich cloud. In either case, the C I–rich cloud would be regarded as a young cloud that is just forming dense cores.

Finally, we briefly discuss dense core formation in the HCL2 region. Dense cores seen in $C^{18}O$ mainly exists in the northern half of HCL2, whereas the C I–rich cloud mainly exists in the southern half. This implies that dense cores have been forming currently from the northern part of HCL2 to the southern part. This direction is consistent with the relative ages proposed for the TMC-1 ridge (Hirahara et al. 1992, 1995); the cyanopolyyne peak is in an earlier stage than the ammonia peak. Thus, the C I observation would provide us with unique and direct information on the formation and structure of the molecular cloud cores.

We are grateful to Kazuyoshi Sunada and Yoshimi Kitamura for allowing us to use the ^{13}CO and $C^{18}O$ maps prior to publication. We are also grateful to Tomoharu Oka for valuable discussion. We thank Katsuhiko Sato and members of RESCEU for various supports to the Mount Fuji submillimeter-wave telescope project. We indebted to Norio Kaifu and Hiroo Inokuchi for continuous encouragement throughout this study. We thank the staff of the Nobeyama Radio Observatory for technical support. This study is supported by a Grant-in-Aid from the Ministry of Education, Science, and Culture (07CE2002).

REFERENCES

Benson, P. J., & Myers, P. C. 1989, ApJS, 71, 89
Boissé, P. 1990, A&A, 228, 483
Burton, M. G., Hollenbach, D. J., & Tielens, A. G. G. M. 1990, ApJ, 365, 620
Cernicharo, J., & Guélin, M. 1987, A&A, 176, 299
Cernicharo, J., Guélin, M., & Askne, J. 1984, A&A, 138, 371
Elias, J. H. 1978, ApJ, 224, 857
Genzel, R., Harris, A. I., Jaffe, D. T., & Stutzki, J. 1988, ApJ, 332, 1049
Heiles, C. E. 1968, ApJ, 151, 919
Hirahara, Y., et al. 1992, ApJ, 394, 539
———. 1995, PASJ, 47, 845
Ikeda, M., et al. 1999, ApJL, submitted
Inatani, J., Shi, S.-C., Sekimoto, Y., Masuko, H., & Ochiai, S. 1998, in Proc. Ninth Int. Symp. Space Terahertz Technology, ed. R. McGrath (Pasadena: JPL), 337
Ingalls, J. G., Chamberlin, R. A., Bania, T. M., Jackson, J. M., Lane, A. P., & Stark, A. A. 1997, ApJ, 479, 296
Itoh, Y., Tamura, M., & Gatley, I. 1996, ApJ, 465, L129
Itoh, Y., Tamura, M., & Nakajima, T. 1999, AJ, 117, 1471
Kaifu, N., et al. 1999, in preparation
Lee, H.-H., Herbst, E., Pineau de Forêts, G., Roueff, E., & Bourlot J. L. 1996, A&A, 311, 690
Leung, C. M., Herbst, E., & Huebner, W. F. 1984, ApJS, 56, 231
Little, L. T., Macdonald, G. H., Riley, P. W., & Matheson, D. N. 1979, MNRAS, 189, 539
Mizuno, A., Onishi, T., Yonekura, Y., Nagahama, T., Ogawa, H., & Fukui, Y. 1995, ApJ, 445, L161
Ohishi, M., Irvine W. M., & Kaifu, N. 1991, in Astrochemistry of Cosmic Phenomena, ed. P. D. Singh (Dordrecht: Kluwer), 171
Olano, C. A., Walmsley, C. M., & Wilson, T. L. 1988, A&A, 196, 194
Onishi, T., Mizuno, A., Kawamura, A., Ogawa, H., & Fukui, Y. 1996, ApJ, 465, 815
———. 1998, ApJ, 502, 296
Plume, R., Jaffe, D. T., Tatematsu, K., Evans, N. J., II, & Keene, J. 1999, ApJ, 512, 768
Pratap, P., Dickens, J. E., Snell, R. L., Miralles, M. P., Bergin, E. A., Irvine, W. M., & Schloerb, F. P. 1997, ApJ, 486, 862
Schilke, P., Keene, J., Bourlot, J. L., Pineau des Forêts, G., & Ruoeff, E. 1995, A&A, 294, L17
Schloerb, F. P., & Snell, R. L. 1984, ApJ, 283, 129
Sekimoto, Y., et al. 1996, Int. J. Infrared Millimeter Waves, 17, 1263
———. 1999, in preparation
Shi, S.-C., Noguchi, T., & Inatani, J. 1997, IEEE Trans. Appl. Supercond., 7, 2587
Snell, R. L., Langer, W. D., & Frerking, M. A. 1982, ApJ, 255, 149
Spaans, M. 1996, A&A, 307, 271
Stark, R., & van Dishoeck, E. F. 1994, A&A, 286, L43
Stark, R., Wesselius, P. R., Van Dishoeck, E. F., & Laureijs, R. J. 1996, A&A, 311, 282
Stutzki, J., Stacey, G. J., Genzel, R., Harris, A. I., Jaffe, D. T., & Lugten, J. B. 1988, ApJ, 332, 379
Sunada, K., & Kitamura, Y. 1999, in preparation
Suzuki, H., Yamamoto, S., Ohishi, M., Kaifu, N., Ishikawa, S., Hirahara, Y., & Takano, S. 1992, ApJ, 392, 551
Tatematsu, K., Jaffe, D. T., Plume, P., Evans, N. J., II, & Keene, J. 1999, ApJ, in press
White, G. J., Casali, M. M., & Eiroa, C. 1995, A&A, 298, 594
Yamamoto, S., & Saito, S. 1991, ApJ, 370, L103